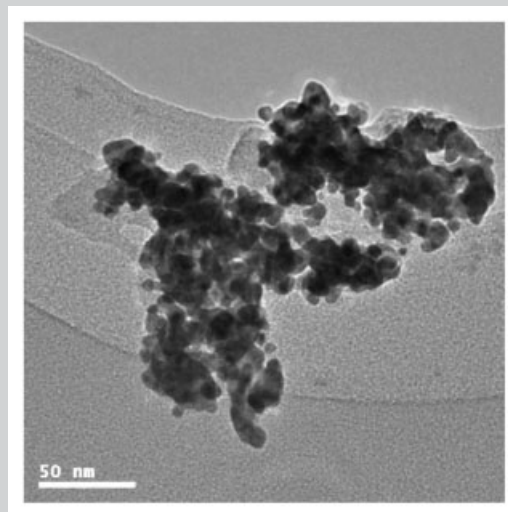


Summary: A water-soluble gold nanoparticle aggregate **2** was prepared by chloroauric acid and a polypseudorotaxane **1** of mono-6-thio- β -cyclodextrin with poly(propylene glycol) bis(2-aminopropyl ether) ($M_w \approx 2000$) in the presence of sodium borohydride in *N,N*-dimethylformamide (DMF) solution. The investigative results indicated that the gold nanoparticle aggregate **2** might act as an efficient DNA-cleavage reagent.



A typical TEM image of gold nanoparticle aggregate **2**.

Supramolecular Assembly of Gold Nanoparticles Mediated by Polypseudorotaxane with Thiolated β -Cyclodextrin^a

Yu Liu,* Yan-Li Zhao, Yong Chen, Min Wang

Department of Chemistry, State Key Laboratory of Elemento-Organic Chemistry, Nankai University, Tianjin 300071, P.R. China
Fax: +86-22-23503625; E-mail: yuliu@public.tpt.tj.cn

Received: October 14, 2004; Revised: December 10, 2004; Accepted: December 20, 2004; DOI: 10.1002/marc.200400476

Keywords: cyclodextrin; nanoparticles; polypseudorotaxane; self-assembly; supramolecular structure

Introduction

Recently, there has been great interest in the rational fabrication of metal nanoparticle aggregates because their electronic, optical, magnetic, and biological properties are distinctly different from those of the corresponding individual nanoparticles.^[1–5] Among the various organic and biomolecules used to functionalize the nanoparticles, such as sulfur-based compounds, proteins,^[6,7] DNA,^[8–12] enzymes,^[13–17] and cyclodextrins,^[17–22] cyclodextrins (CDs), a series of cyclic saccharides possessing a hydrophobic inner cavity and a hydrophilic outer wall, are regarded as one of

the best choices because of their high solubilization ability, low toxicity, and specific recognition ability towards many model substrates. Kaifer and coworkers,^[18] Matsui and coworkers,^[19] and Reinhoudt and coworkers^[20] separately reported the preparation of thioCD-modified gold nanoparticles (AuNPs) and their supramolecular aggregates, which showed significant phase transfer and catalytic properties. However, the general methodology employed in these studies mainly focused on assembling the discrete CD-modified nanoparticles into supramolecular aggregates by interparticle 2:1 inclusion complexation between the CD cavities and various bridge agents, such as ferrocene,^[18a,c] fullerene,^[18e] and phenanthroline^[23] etc., the covalently linked aggregates of nanoparticles have been rarely reported so far, to the best of our knowledge. On the other hand, the syntheses of a series of polyrotaxanes/polypseudorotaxanes, which could serve as the building blocks of

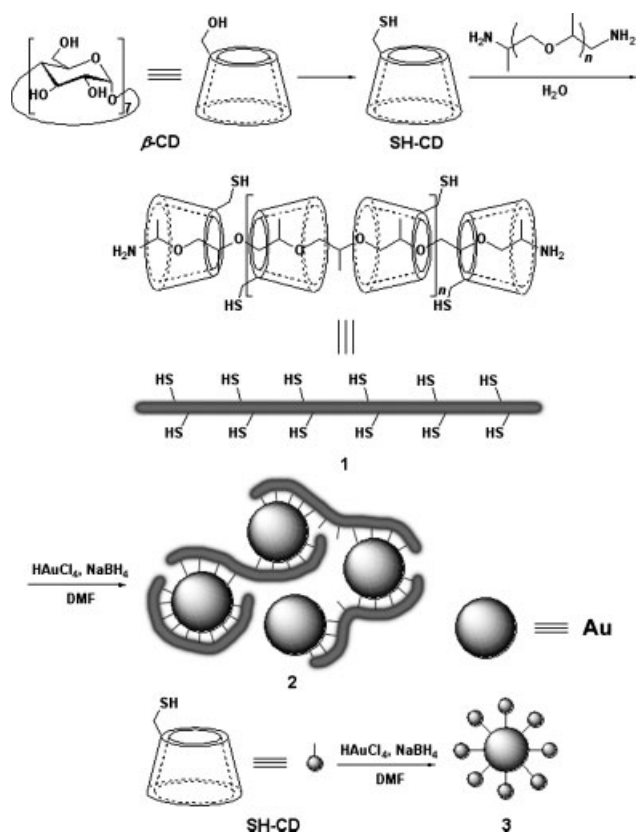
^a Supporting information for this article is available at the bottom of the article's abstract page, which can be accessed from the journal's homepage at <http://www.mrc-journal.de>, or from the author.

molecular machines and functional materials, were recently reported.^[24–28] In this work, we synthesize a new poly(propylene glycol) bis(2-aminopropylether) (PPG)-threaded polypseudorotaxane based on mono-6-thio- β -CD (SH-CD). Subsequently, the gold nanoparticles (AuNPs) are covalently grafted to the polypseudorotaxane through the Au–S combinations to form water-soluble AuNP aggregates (**2**), which are comprehensively characterized by UV-vis, ¹H NMR, and FT-IR spectroscopy, powder X-ray diffraction (XRD), and transmission electron microscopy (TEM). Because of the presence of many Au–S bonds in the AuNP aggregates **2**, the aggregates exhibit good photoinduced DNA-cleavage ability through the sulfur-to-gold charge transfer and gold d–d transition. Therefore, our current work provides not only a new method for the construction of metal nanoparticle aggregates but also a potential hybrid material with good biological functions.

Results and Discussion

Synthesis

The synthesis route to obtain an AuNP aggregate **2** is shown in Scheme 1. Firstly, SH-CD^[29] was threaded onto poly(propylene glycol) bis(2-aminopropylether) (PPG-



Scheme 1. Synthetic route of AuNP aggregation **2**.

NH₂, $\overline{M}_w \approx 2000$) to give polypseudorotaxane **1**, and the further reaction of **1** with chloroauric acid (HAuCl₄) in the presence of sodium borohydride (NaBH₄) in *N,N*-dimethylformamide (DMF) solution gave the AuNP aggregate **2** in 68% yield through the adsorption of hydrosulfide groups of SH-CDs onto the surface of AuNPs. In the control experiment, the thioCD-modified AuNP **3** was also synthesized in 73% yield as a reference compound by the reaction of SH-CD with AuNP. Because of the polarity of the hydroxyl groups in the SH-CD units, which afforded a polar character to the surface of the AuNPs,^[18b] **2** displayed a moderate water solubility up to 0.25 mg · mL⁻¹.

UV-Vis, FT-IR, and NMR Spectra

As compared with the UV-vis spectra of AuNPs^[30] and **3** in aqueous solution, which show characteristic absorptions at 520 and at 532 nm, respectively, for the surface plasmon resonance (SPR) absorption, the SPR maximum of **2** (0.15 mg mL⁻¹) is obviously shifted to ca. 610 nm. In addition, the FT-IR spectrum of **2** was found to be fairly similar to that of **1**, except that the intensity of the S–H stretching band at ca. 2 143 cm⁻¹ in the IR spectrum of **1** significantly decreased after reacting **1** with AuNPs. This indicated that most of the –SH groups were consumed during the formation of **2**. Moreover, the absorption intensities of IR bands at ca. 2 899 and 3 312 cm⁻¹ in the IR spectrum of **1**, which were assigned to the stretching vibration of C–H and O–H groups, respectively, in SH-CDs, also significantly decreased after reacting **1** with AuNPs. According to the reference results,^[18a,b] the decrease of these two IR bands may be attributed to the formation of gold nanoparticle aggregates. Furthermore, the ¹H NMR experiments of **1** and **2** also provided information about their possible structure. From the ¹H NMR spectrum of **1** in DMSO-*d*₆, a comparison of the integral area of proton peaks indicated that the ratio between PPG-NH₂'s methyl protons (a molecule of PPG-NH₂ 2000 contains ca. 34 methyl protons, $\delta = 1.03$ – 1.05 (d)) and SH-CD's H-1 protons (a molecule of SH-CD contains 7 H-1 protons, $\delta = 4.84$ (s)) was 7.7:7.0. In the case of **2**, this ratio between PPG-NH₂'s methyl protons ($\delta = 0.84$ – 0.89 (m)) and SH-CD's H-1 protons ($\delta = 4.83$ (s)) was 8.7:7.0. According to these ¹H NMR data, we could calculate that, for **1**, one PPG-NH₂ molecule could thread ca. 13 SH-CD units, and for **2**, about 12 SH-CD units. To further confirm the threading of SH-CDs onto PPG-NH₂, the ROESY experiment of **1** was performed. Because of the relatively low water solubility of **1**, a DMSO-*d*₆/D₂O (v:v = 1:4) solution was used in the two-dimensional NMR experiments. As illustrated in Figure 1, the ROESY spectrum showed clear nuclear Overhauser effect (NOE) correlations (peaks A) between the methyl protons of PPG-NH₂ and the H5/H6 protons of SH-CDs. Because the H5 and H6 protons are located in the interior and edge of the cyclodextrin cavity, respectively, these NOE correlations

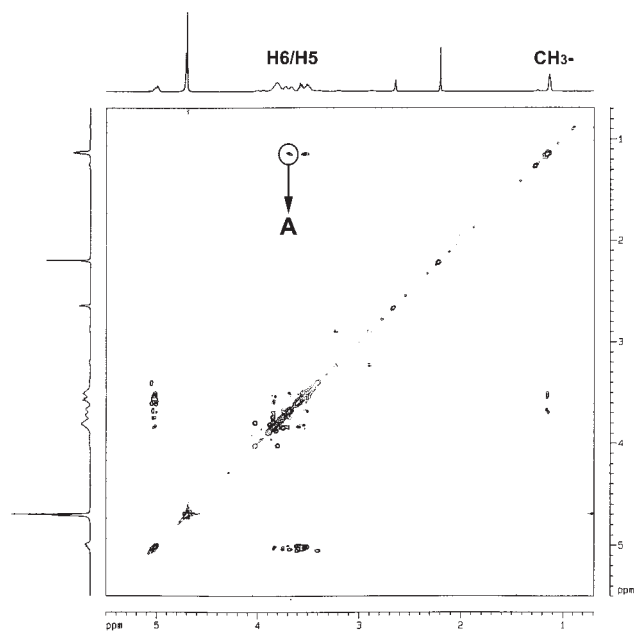


Figure 1. Two-dimensional ROESY spectrum of polypseudorotaxane **1** ($2 \text{ mg} \cdot \text{mL}^{-1}$) in a $\text{DMSO-}d_6/\text{D}_2\text{O}$ ($v:v = 1:4$) solution at 25°C with a mixing time of 200 ms.

demonstrate that the PPG-NH₂ was threaded into the SH-CD cavities to form a polypseudorotaxane.^[24b] Moreover, the ¹H NMR spectrum of **2** in D₂O showed that the signals for the nanoparticle-immobilized CDs were broadened. This phenomenon was similar to that reported by Kaifer and coworkers,^[18] and the fast relaxation and environmental heterogeneities were thought to be responsible for these line broadening effects. From the UV-vis, FT-IR, and ¹H NMR evidence mentioned above, we could conclude that the SH-CDs in the polypseudorotaxanes were attached to the surface of the AuNPs.

Transmission Electron Microscopy

Transmission electron microscopy (TEM) has become a convenient and widely employed method for the elucidation of certain microstructures of nanoparticle aggregates. Figure 2 gave a typical high-resolution TEM image of **3**, showing numerous discrete nanoparticles with an average diameter of $4.8 \pm 2.1 \text{ nm}$. Interestingly, the TEM image of **2** exhibited an entirely different arrangement mode from that of **3**, displaying an agglomerate assembly as shown in Figure 3. According to the high-resolution TEM image of **2**, the average diameters of AuNPs and their aggregates were about $5.2 \pm 2.0 \text{ nm}$ and $70 \pm 10 \text{ nm}$, respectively, which clearly indicated the aggregation of AuNPs through the linkage of CD-based polypseudorotaxanes.

Powder X-Ray Diffraction

The XRD pattern of a sample could probe a large number of crystallites that are statistically oriented. Figure 4 illustrates the wide-angle X-ray diffraction patterns of SH-CD, polypseudorotaxane **1**, aggregate **2**, and the parent AuNPs. As seen from Figure 4, the diffractogram of SH-CD shows several characteristic reflections at $2\theta = 12.5^\circ$ ($d = 7.09 \text{ \AA}$), 15.4° (5.74 \AA), 17.2° (5.16 \AA), 18.8° (4.71 \AA), and 22.7° (3.91 \AA), but these reflections changed to $2\theta = 11.8^\circ$ ($d = 7.52 \text{ \AA}$), 15.2° (5.84 \AA), 17.6° (5.04 \AA), 20.0° (4.43 \AA), and 23.8° (3.74 \AA) in the diffractogram of **1**, indicating that the arrangement of SH-CD in **1** was changed by the introduction of PPG-NH₂. Furthermore, four characteristic reflections around $2\theta = 38.1^\circ$ ($d = 2.35 \text{ \AA}$), 44.4° (2.03 \AA), 64.7° (1.45 \AA), and 77.6° (1.23 \AA), which correspond to the (111) (200) (220), and (311) planes of the cubic phase of Au in the diffractogram of the parent AuNPs are slightly shifted to ca. $2\theta = 38.2^\circ$ ($d = 2.36 \text{ \AA}$), 44.3° (2.04 \AA), 64.6° (1.44 \AA), and 77.7° (1.23 \AA) in the diffractogram of **2**. Moreover, the reflections around $2\theta = 18.7^\circ$

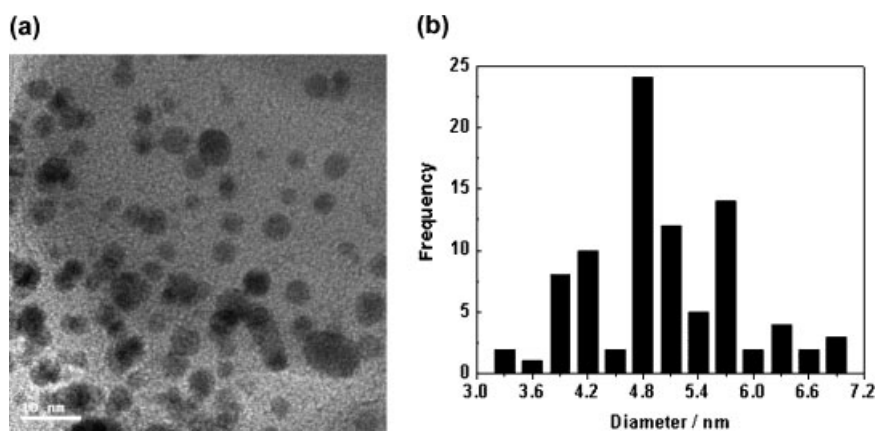


Figure 2. (a) High-resolution TEM image of **3**, and (b) size-dependent histograms for AuNPs **3**.

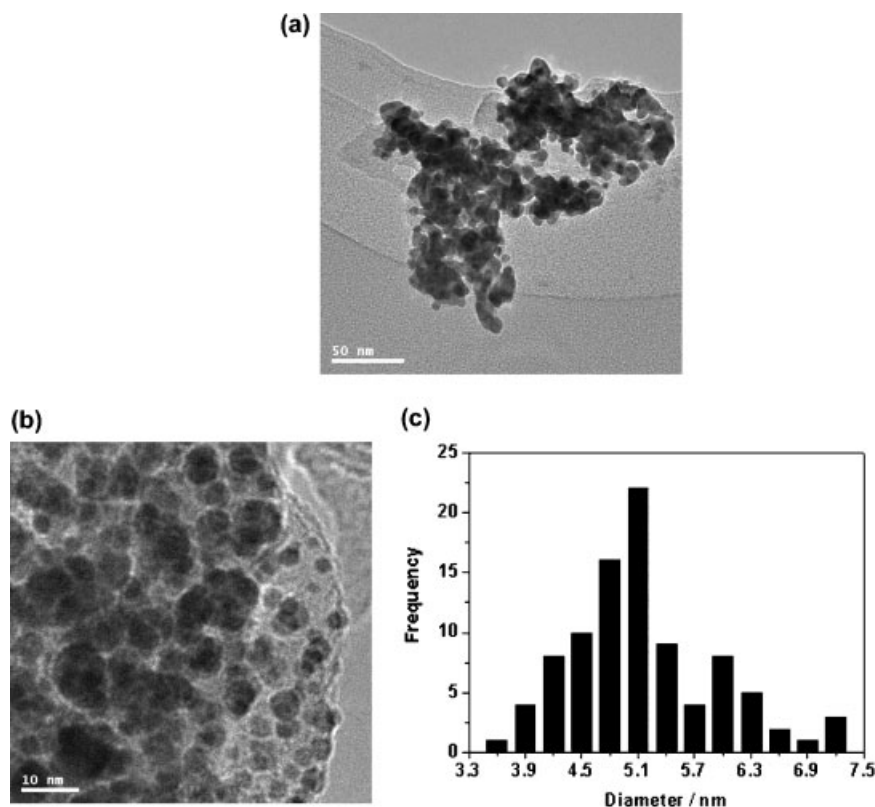


Figure 3. (a) Typical TEM and (b) high-resolution TEM images of **2**, and (c) size-dependent histograms for AuNPs in aggregate **2**.

($d = 4.75 \text{ \AA}$) and 28.4° (3.14 \AA) in the diffractogram of the AuNPs disappeared after reacting **1** with the AuNPs, and a new reflection around $2\theta = 31.7^\circ$ ($d = 2.82 \text{ \AA}$) appeared in the diffractogram of **2**. It is well documented that the introduction of modified groups will change the arrangement mode of AuNPs to some extent and thus produce an XRD pattern different from that of the parent AuNPs.^[31,32] Therefore, these phenomena jointly indicated that polypseudorotaxane **1** was combined with AuNPs. In addition, the average size of the AuNPs could also be determined from the width of reflection according to the Scherrer

formula $D = 0.9\lambda/(\beta \cos\theta)$, where β was the full width at the half-maximum height of the peak, θ was the angle of diffraction, and λ was the wavelength of X-ray radiation.^[33,34] The resultant value of D calculated from the (111) reflection of the cubic phase of Au in **2** was ca. 5.0 nm, which was in good agreement with the TEM investigation results.

DNA Cleavage

It is significant to note that the water-soluble AuNP **2** showed good DNA-cleavage abilities at 25°C . As shown in Figure 5, ca. 75% of the closed supercoiled pBR322 DNA (form I) were cleaved to the nicked DNA (form II) under visible-light irradiation in the presence of **2**. In control experiments, neither SH-CD nor polypseudorotaxane **1** displayed an appreciable DNA-cleavage ability under our experimental conditions. Chakravarty and coworkers have reported a photoinduced DNA-cleavage mechanism for the Cu–S complexes.^[35] In this mechanism, both the sulfur-to-copper charge-transfer band and the copper d–d band excitations are responsible for the DNA cleavage. That is, while the absorption of a red light induced a metal d–d transition, the excitation at shorter visible wavelengths led to the sulfur-to-copper charge-transfer band excitation at the initial step of photocleavage. The excitation energy is

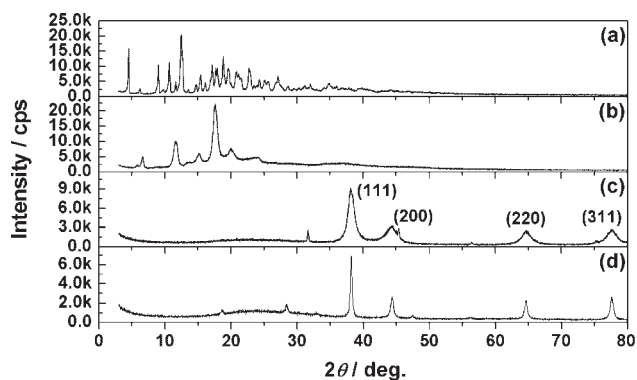


Figure 4. XRD patterns of (a) SH-CD, (b) polypseudorotaxane **1**, (c) AuNP aggregate **2**, and (d) parent AuNPs.

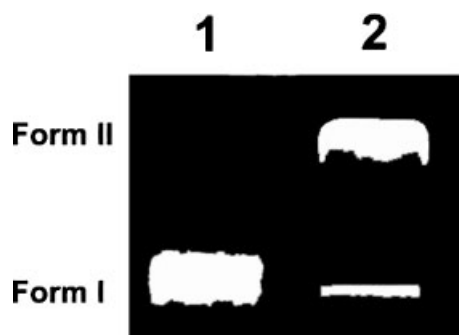


Figure 5. DNA-cleavage ability of **2** in phosphate buffer (50×10^{-3} M, pH 7.4) at 25 °C. 1: DNA, 2: DNA + **2**. [**2**] = $0.04 \text{ mg} \cdot \text{mL}^{-1}$, [DNA] = $0.004 \text{ } \mu\text{g} \cdot \text{mL}^{-1}$.

subsequently transferred to ground state oxygen molecules to produce the singlet oxygen that cleaved the DNA. Because gold and copper were congeners, we deduce that the DNA-cleavage mechanism for the thioCD-modified AuNP aggregate **2** should be similar to that for the Cu–S systems.

Conclusion

In conclusion, we have presented a water-soluble nanoparticle aggregate obtained by the molecular assembly of AuNPs and polypseudorotaxanes. The introduction of polypseudorotaxanes with mono-6-thio- β -CD resulted in a novel assembly behavior for the nanoparticles. Furthermore, the nanoparticle aggregate could act as an efficient DNA-cleavage reagent, which is attractive for biological applications, especially upon taking into account the versatility of the molecular assembly approach for surface derivatization.

Experimental Part

Materials

β -Cyclodextrin (β -CD) of reagent grade (Shanghai Reagent Factory) was recrystallized twice from water and dried under vacuum at 95 °C for 24 h prior to use. *N,N*-Dimethylformamide (DMF) was dried over calcium hydride for two days and then distilled under reduced pressure prior to use. Poly(propylene glycol) bis(2-aminopropylether) (PPG-NH₂, $\bar{M}_w \approx 2000$), chloroauric acid (HAuCl₄), sodium borohydride (NaBH₄), and DNA pBR322 were commercially available and used without further purification. Mono-6-thio- β -CD (SH-CD)^[29] and the parent gold nanoparticles (AuNPs)^[30] were prepared according to previous reports, as indicated.

Instruments

¹H NMR spectra were recorded in D₂O or DMSO-*d*₆ on a Varian Mercury VX300 spectrometer. NOESY spectra were recorded in DMSO-*d*₆/D₂O (v:v = 1:4) on a Bruker AV600

spectrometer. UV-Vis spectra were recorded in a conventional quartz cell (light path 10 mm) on a Shimadzu UV-2401PC spectrophotometer equipped with a PTC-348WI temperature controller to maintain the temperature at 25 °C. FT-IR spectra were recorded on a Bio-Rad FTS 135 infrared spectrometer. The powder X-ray diffraction (XRD) patterns were obtained using a Rigaku D/max-2500 diffractometer with Cu K α radiation ($\lambda = 1.5405 \text{ \AA}$). Transmission electron microscopy (TEM) experiments were performed using a Philips Tecnai G² 20 S-TWIN microscope operating at 200 kV. TEM samples were prepared by depositing a drop of the suspension onto a perforated carbon grid.

Synthesis of Polypseudorotaxane **1**

PPG-NH₂ (20.0 mg) was added dropwise to a saturated aqueous solution (40 mL) containing 94.0 mg of SH-CD, and the mixture was stirred for 10 h and then allowed to stand overnight at room temperature. The formed precipitate was collected by centrifugation, washed with THF, and then dried under vacuum to give the polypseudorotaxane **1**. Data for **1**: yield 62%. ¹H NMR (300 MHz, DMSO-*d*₆, TMS, ppm): $\delta = 1.03\text{--}1.05$ (d, 7.7H), 3.27–3.63 (m, H), 4.44–4.48 (m, 7H), 4.84 (s, 7H), 5.69–5.78 (m, 14H). FT-IR (KBr): 3342.6, 2910.6, 2142.9, 1641.4, 1433.1, 1367.2, 1156.3, 1076.9, 1027.6, 944.4, 851.5, 755.1, 704.7, 584.4 cm⁻¹. Powder X-ray diffraction (XRD): $2\theta = 6.6^\circ$ (*d* 13.30 Å), 11.8 (7.52), 15.2 (5.84), 17.6 (5.04), 20.0 (4.43), 23.8 (3.74), 37.1 (2.42).

Synthesis of AuNP Aggregate **2**

Equal volumes (20 mL) of HAuCl₄ (50 mg) in DMF and a second DMF solution containing NaBH₄ (75.5 mg) and polypseudorotaxane **1** (36.8 mg) were quickly mixed, and the solution became deep brown immediately. The resultant mixture was stirred at room temperature for 24 h. The precipitate formed was collected by centrifugation and was washed with DMF (4 \times 50 mL) to remove free polypseudorotaxane **1**. The obtained solid product was further washed (4 \times 50 mL) with ethanol/water (90:10 v/v), collected by centrifugation, and then dried under vacuum to give **2**. Data for **2**: yield 68%. ¹H NMR (300 MHz, DMSO-*d*₆, TMS, ppm): $\delta = 0.84\text{--}0.89$ (d, 8.7H), 3.22–3.64 (m, H), 4.44–4.48 (m, 6H), 4.83 (s, 7H), 5.69–5.79 (m, 14H). ¹H NMR (300 MHz, D₂O, TMS, ppm): $\delta = 0.67\text{--}0.72$ (d, 8.6H), 3.13–3.80 (m, H), 4.87–4.98 (m, 7H). FT-IR (KBr): 3311.7, 2899.0, 1662.6, 1442.8, 1329.4, 1157.2, 1032.0, 960.5, 715.6, 597.9 cm⁻¹. Powder X-ray diffraction (XRD): $2\theta = 31.7^\circ$ (*d* 2.82 Å), 38.2 (2.36), 44.3 (2.04), 64.6 (1.44), 77.7 (1.23).

Synthesis of AuNP **3**

Similar to that in the previous reports,^[18b,23] equal volumes (20 mL) of HAuCl₄ (50 mg) in DMF and a second DMF solution containing NaBH₄ (75.5 mg) and SH-CD (30.0 mg) were quickly mixed, and the solution became deep brown immediately. The resultant mixture was stirred at room temperature for 24 h. The precipitate formed was collected by centrifugation and washed with DMF (4 \times 50 mL) to remove

free SH-CD. The obtained solid product was further washed (4×50 mL) with ethanol/water (90:10 V/V), collected by centrifugation, and then dried under vacuum to give **3**. Data for **3**: yield 73%. $^1\text{H NMR}$ (300 MHz, D_2O , TMS, ppm): $\delta = 3.10\text{--}4.18$ (m, 41H), 4.89–5.13 (m, 7H). FT-IR (KBr): 3327.9, 2900.1, 1671.2, 1436.0, 1337.7, 1156.0, 1031.9, 950.5, 878.6, 755.6, 708.6, 580.7, 530.3 cm^{-1} .

Examination of DNA-cleavage Ability

An aqueous solution (10 μL) of pBR322 DNA ($0.51 \mu\text{g} \cdot \mu\text{L}^{-1}$) was diluted by adding 90 μL of water. An aqueous solution of **2** (10 μL , $0.2 \text{ mg} \cdot \text{mL}^{-1}$), 12 μL of an aqueous solution of pBR322 DNA ($0.051 \mu\text{g} \cdot \mu\text{L}^{-1}$), and 8 μL of a phosphate buffer ($250 \times 10^{-3} \text{ M}$, pH 7.4) were mixed in a micro test tube under dark conditions to give the sample solution. Aliquots of the sample (20 μL) were incubated under irradiation with a 300 W reflector lamp for 1 h at 298 K, and then mixed with 4 μL of $6 \times$ loading buffer, and loaded onto a 1% agarose gel containing ethidium bromide ($10 \mu\text{g} \cdot \text{mL}^{-1}$). The gels were run at a constant voltage of 80 V for 1 h in TAE (Tris-Acetate-EDTA) buffer, washed with distilled water, visualized under a UV transilluminator, and photographed using an instant camera.

Acknowledgements: This work was supported by NNSFC (Nos. 90306009, 20272028, and 20402008) and the Tianjin Natural Science Fund (No. 043604411), which are gratefully acknowledged.

- [1] M.-C. Daniel, D. Astruc, *Chem. Rev.* **2004**, *104*, 293.
- [2] A. C. Templeton, W. P. Wuelfing, R. W. Murray, *Acc. Chem. Res.* **2000**, *33*, 27.
- [3] K. G. Thomas, P. V. Kamat, *Acc. Chem. Res.* **2003**, *36*, 888.
- [4] [4a] C. M. Niemeyer, *Angew. Chem. Int. Ed.* **2001**, *40*, 4128; [4b] C. M. Niemeyer, *Angew. Chem. Int. Ed.* **2003**, *42*, 5796.
- [5] J. Liu, J. Alvarez, A. E. Kaifer, *Adv. Mater.* **2000**, *12*, 1381.
- [6] [6a] W. C. W. Chan, S. Nie, *Science* **1998**, *281*, 2016; [6b] D. J. Maxwell, J. R. Taylor, S. Nie, *J. Am. Chem. Soc.* **2002**, *124*, 9606.
- [7] [7a] H. Mattoussi, J. M. Mauro, E. R. Goldman, G. P. Anderson, V. C. Sundar, F. V. Mikulec, M. G. Bawendi, *J. Am. Chem. Soc.* **2000**, *122*, 12142; [7b] A. R. Clapp, I. L. Medintz, J. M. Mauro, B. R. Fisher, M. G. Bawendi, H. Mattoussi, *J. Am. Chem. Soc.* **2004**, *126*, 301.
- [8] K. Sato, K. Hosokawa, M. Maeda, *J. Am. Chem. Soc.* **2003**, *125*, 8102.
- [9] J. Liu, Y. Lu, *J. Am. Chem. Soc.* **2003**, *125*, 6642.
- [10] [10a] R. Elghanian, J. J. Storhoff, R. C. Mucic, R. L. Letsinger, C. A. Mirkin, *Science* **1997**, *277*, 1078; [10b] S.-J. Park, A. A. Lazarides, C. A. Mirkin, P. W. Brazis, C. R. Kannewurf, R. L. Letsinger, *Angew. Chem. Int. Ed.* **2000**, *39*, 3845; [10c] J. J. Storhoff, A. A. Lazarides, R. C. Mucic, C. A. Mirkin, R. L. Letsinger, G. C. Schatz, *J. Am. Chem. Soc.* **2000**, *122*, 4640; [10d] R. Jin, G. Wu, Z. Li, C. A. Mirkin, G. C. Schatz, *J. Am. Chem. Soc.* **2003**, *125*, 1643.
- [11] C. M. Niemeyer, B. Ceyhan, P. Hazarika, *Angew. Chem. Int. Ed.* **2003**, *42*, 5766.
- [12] A. G. Tkachenko, H. Xie, D. Coleman, W. Glomm, J. Ryan, M. F. Anderson, S. Franzen, D. L. Feldheim, *J. Am. Chem. Soc.* **2003**, *125*, 4700.
- [13] A. G. Kanaras, Z. Wang, A. D. Bates, R. Cosstick, M. Brust, *Angew. Chem. Int. Ed.* **2003**, *42*, 191.
- [14] C. S. Yun, G. A. Khitrov, D. E. Vergona, N. O. Reich, G. F. Strouse, *J. Am. Chem. Soc.* **2002**, *124*, 7644.
- [15] V. Pardo-Yissar, E. Katz, J. Wasserman, I. Willner, *J. Am. Chem. Soc.* **2003**, *125*, 622.
- [16] S. R. N. Peña, S. Raina, G. P. Goodrich, N. V. Fedoroff, C. D. Keating, *J. Am. Chem. Soc.* **2002**, *124*, 7314.
- [17] A. Taden, M. Antonietti, K. Landfester, *Macromol. Rapid Commun.* **2003**, *24*, 512.
- [18] [18a] J. Liu, S. Mendoza, E. Román, M. J. Lynn, R. Xu, A. E. Kaifer, *J. Am. Chem. Soc.* **1999**, *121*, 4304; [18b] J. Liu, J. Alvarez, W. Ong, E. Román, A. E. Kaifer, *J. Am. Chem. Soc.* **2001**, *123*, 11148; [18c] L. Strimbu, J. Liu, A. E. Kaifer, *Langmuir* **2003**, *19*, 483; [18d] J. Liu, J. Alvarez, W. Ong, A. E. Kaifer, *Nano Lett.* **2001**, *1*, 57.
- [19] I. A. Banerjee, L. Yu, H. Matsui, *J. Am. Chem. Soc.* **2003**, *125*, 9542.
- [20] [20a] J. Huskens, M. A. Deij, D. N. Reinhoudt, *Angew. Chem. Int. Ed.* **2002**, *41*, 4467; [20b] M. R. de Jong, J. Huskens, D. N. Reinhoudt, *Chem. Eur. J.* **2001**, *7*, 4164.
- [21] R. C. Sabapathy, S. Bhattacharyya, W. E. Cleland, Jr., C. L. Hussey, *Langmuir* **1998**, *14*, 3797.
- [22] N. Lala, S. P. Lalbegi, S. D. Adyanthaya, M. Sastry, *Langmuir* **2001**, *17*, 3766.
- [23] Y. Liu, S.-H. Song, Y.-W. Yang, Y. Chen, *J. Chem. Research* **2004**, 152.
- [24] [24a] Y. Liu, Y.-L. Zhao, H.-Y. Zhang, H.-B. Song, *Angew. Chem. Int. Ed.* **2003**, *42*, 3260; [24b] Y. Liu, L. Li, H.-Y. Zhang, Y.-L. Zhao, X. Wu, *Macromolecules* **2002**, *35*, 9934; [24c] Y. Liu, Y.-L. Zhao, H.-Y. Zhang, X.-Y. Li, P. Liang, X.-Z. Zhang, J.-J. Xu, *Macromolecules* **2004**, *37*, 6362.
- [25] [25a] X. Shuai, F. E. Porbeni, M. Wei, T. Bullions, A. E. Tonelli, *Macromolecules* **2002**, *35*, 2401; [25b] T. Uyar, M. Rusa, A. E. Tonelli, *Macromol. Rapid Commun.* **2004**, *25*, 1382.
- [26] [26a] A. Harada, M. Okada, J. Li, M. Kamachi, *Macromolecules* **1995**, *28*, 8406; [26b] S. Kamitori, O. Matsuzaka, S. Kondo, S. Muraoka, K. Okuyama, K. Noguchi, M. Okada, A. Harada, *Macromolecules* **2000**, *33*, 1500; [26c] T. Michishita, Y. Takashima, A. Harada, *Macromol. Rapid Commun.* **2004**, *25*, 1159.
- [27] [27a] T. Ikeda, T. Ooya, N. Yui, *Macromol. Rapid Commun.* **2000**, *21*, 1257; [27b] T. Nakama, T. Ooya, N. Yui, *Macromol. Rapid Commun.* **2004**, *25*, 739.
- [28] [28a] J. Storsberg, M. Hartenstein, A. H. E. Müller, H. Ritter, *Macromol. Rapid Commun.* **2000**, *21*, 1342; [28b] S.-W. Choi, H. Ritter, *Macromol. Rapid Commun.* **2004**, *25*, 716.
- [29] K. Fujita, T. Ueda, T. Imoto, I. Tabushi, N. Toh, T. Koga, *Bioorg. Chem.* **1982**, *11*, 72.
- [30] K. C. Grabar, R. G. Freeman, M. B. Hommer, M. J. Natan, *Anal. Chem.* **1995**, *67*, 735.
- [31] D. V. Leff, L. Brandt, J. R. Heath, *Langmuir* **1996**, *12*, 4723.
- [32] T. G. Schaaff, M. N. Shafiqullin, J. T. Khoury, I. Vezmar, R. L. Whetten, W. G. Cullen, P. N. First, C. Gutiérrez-Wing, J. Ascensio, M. J. Jose-Yacamán, *J. Phys. Chem. B* **1997**, *101*, 7885.
- [33] P. Zhang, J. Li, D. Liu, Y. Qin, Z.-X. Guo, D. Zhu, *Langmuir* **2004**, *20*, 1466.
- [34] D. V. Leff, P. C. O'hara, J. R. Heath, W. M. Gelbart, *J. Phys. Chem.* **1995**, *99*, 7036.
- [35] S. Dhar, D. Senapati, P. K. Das, P. Chattopadhyay, M. Nethaji, A. R. Chakravarty, *J. Am. Chem. Soc.* **2003**, *125*, 12118.